

## 2D Inverse Dynamic Gait Analysis

### Problem Description

The analysis of captured motion data is addressed in this benchmark by means of an inverse dynamic analysis. This approach is used to calculate the driver torques that the musculoskeletal system generates during human locomotion from acquired kinematic data, foot-ground contact forces and estimated body segment parameters (BSP).

The subject selected to perform the experiments is a healthy adult male, 27 years old, mass 84 kg and height 1,75 m. He walks on a walkway that encloses two force plates (AMTI, AccuGait sampling at 100 Hz). The motion is captured by 12 optical cameras (Natural Point, OptiTrack FLEX:V100 also sampling at 100 Hz) that compute the position of 37 optical markers (See Figure 1).

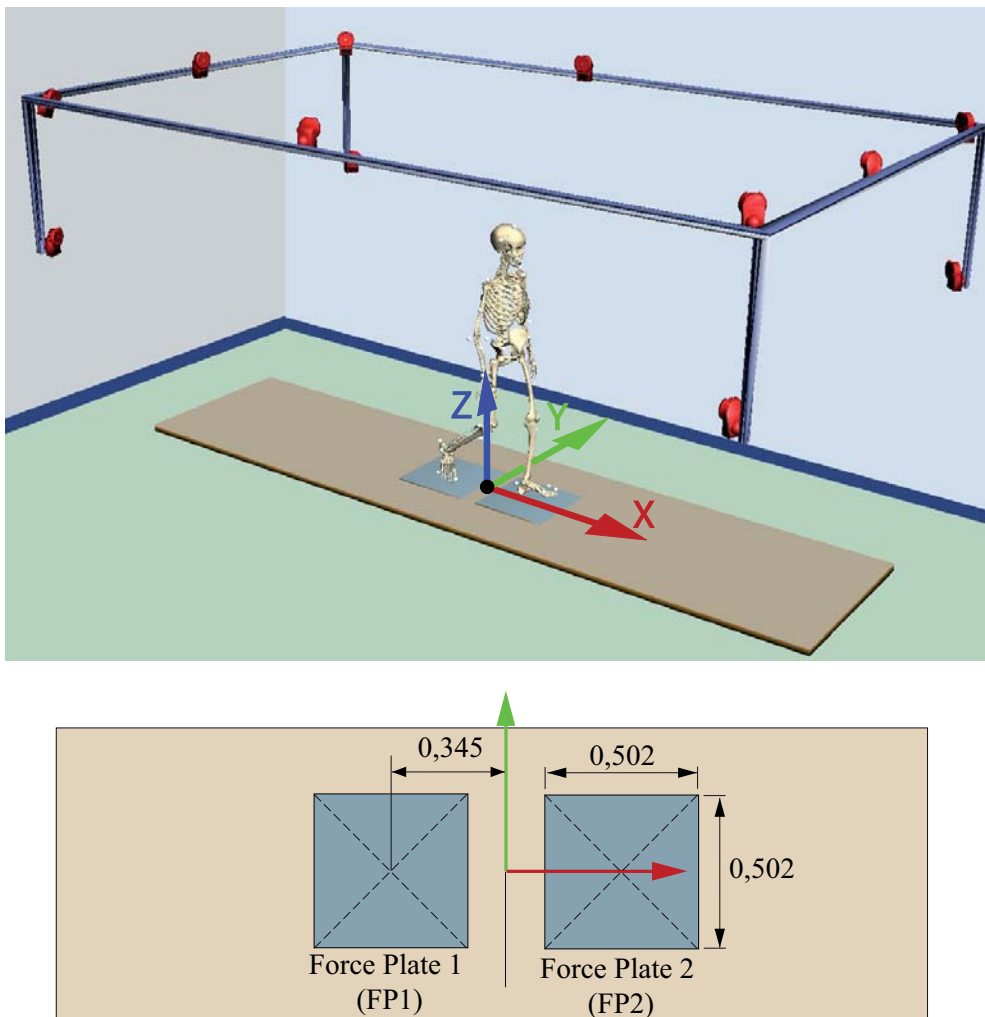
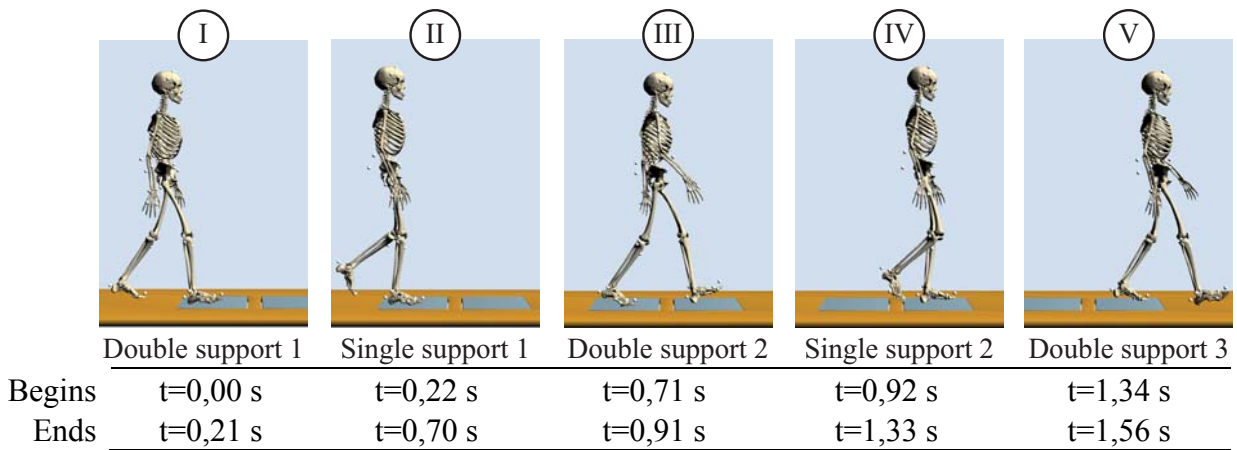


Figure 1. Gait analysis laboratory configuration.

Marker positions are expressed in the global coordinate system, which is defined using the axes  $\{X, Y, Z\}$  (Figure 1). Each force plate registers the ground reactions on one foot during the gait cycle, obtaining as a result a force (three components) and a moment about the centre of the plate (also three components).

Captured data contain information from the 5 gait phases shown in Figure 2.



**Figure 2. Phases of the captured gait motion.**

Figure 3 shows the position of the 37 markers used, and Table 1 contains the anatomical points used to place the markers.

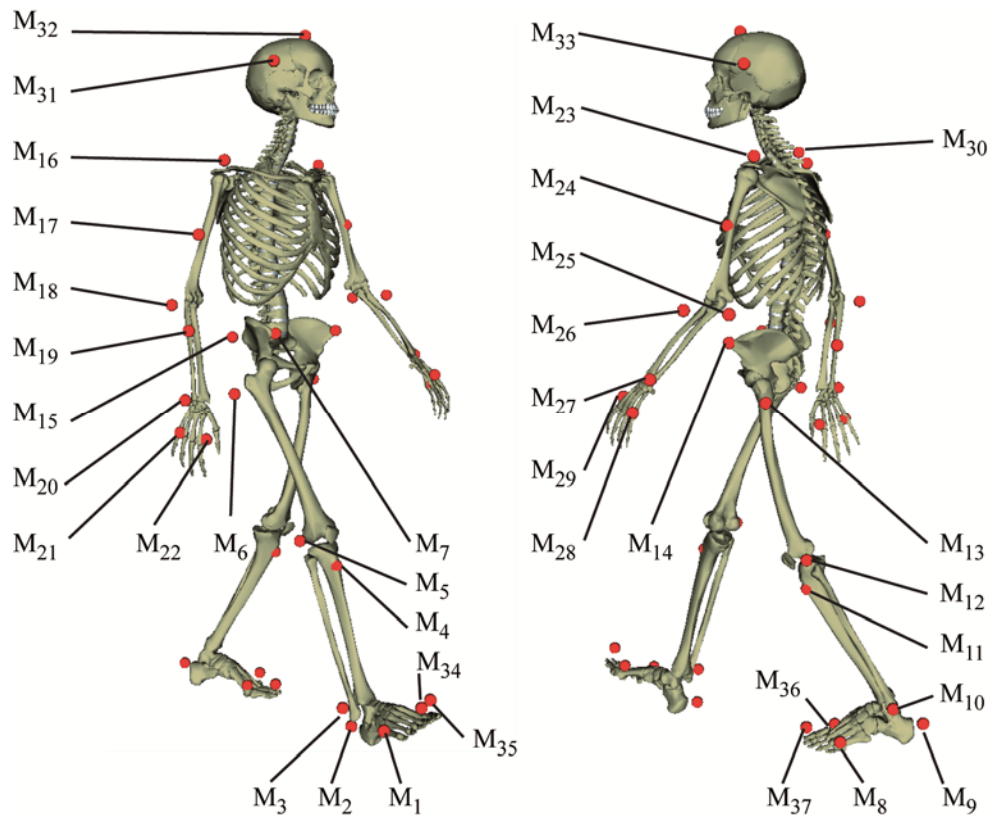


**Figure 3. 3D view of the human skeleton with the set of 37 markers used.**

Symbol	Placement	Symbol	Placement
$M_1$	Right metatarsal head V	$M_8$	Left metatarsal head V
$M_2$	Right calcaneus	$M_9$	Left calcaneus
$M_3$	Right lateral malleolus	$M_{10}$	Left lateral malleolus
$M_4$	Right tibial tuberosity	$M_{11}$	Left tibial tuberosity
$M_5$	Right lateral femoral epicondyle	$M_{12}$	Left lateral femoral epicondyle
$M_6$	Right femoral greater trochanter	$M_{13}$	Left femoral greater trochanter
$M_7$	Right ASIS	$M_{14}$	Left ASIS
$M_{15}$	Sacrum		
$M_{16}$	Right acromion in the shoulder girdle	$M_{23}$	Left acromion in the shoulder girdle
$M_{17}$	Right deltoid tuberosity	$M_{24}$	Left deltoid tuberosity
$M_{18}$	Right lateral humeral epicondyle	$M_{25}$	Left lateral humeral epicondyle
$M_{19}$	Middle of right forearm	$M_{26}$	Middle of left forearm
$M_{20}$	Right radial styloid in the wrist	$M_{27}$	Left radial styloid in the wrist
$M_{21}$	Right metacarpal head V	$M_{28}$	Left metacarpal head V
$M_{22}$	Right metacarpal head II	$M_{29}$	Left metacarpal head II
$M_{30}$	1 <sup>st</sup> vertebra of the thoracic spine		
$M_{31}$	Right side of the head	$M_{33}$	Left side of the head
$M_{32}$	Top of the head		
$M_{34}$	Right metatarsal head I	$M_{36}$	Left metatarsal head I
$M_{35}$	Right distal phalange of the third toe	$M_{37}$	Left distal phalange of the third toe

**Table 1. Placement of the set of markers used.**

The human body is represented by a 12-segment 2D model (Figure 4) with 14 degrees of freedom. The anthropometric parameters can be seen in Table 2, being also available in the text file “Anthropometry.dat” (miscellaneous file). It should be noted that the moment of inertia of the segments is expressed with respect to their COM.

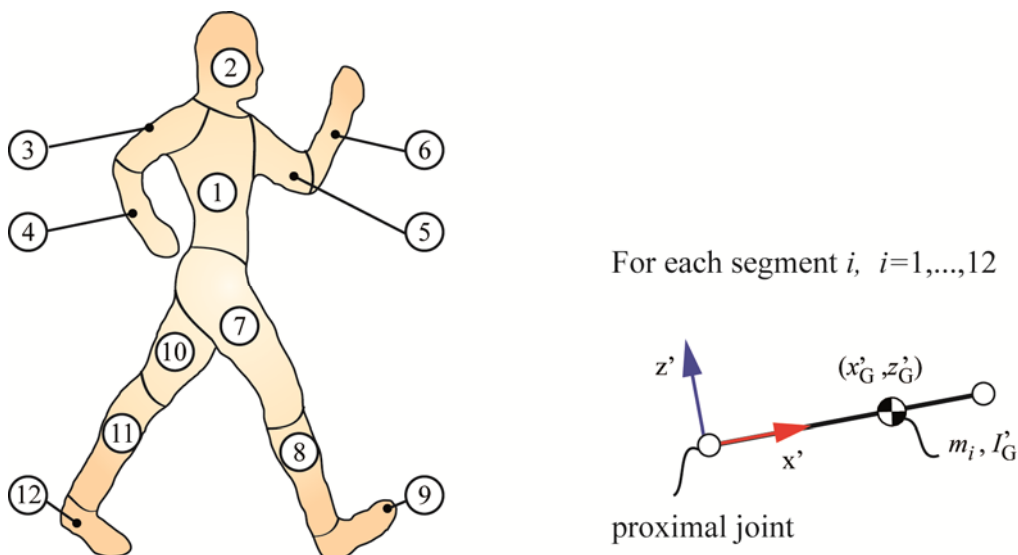


**Figure 4. 2D biomechanical model of the human body.**

No.	Name	Length $L_i$ [m]	COM Location		Mass $m_i$ [kg]	Principal Moment of Inertia $I_G'$ [ $10^{-2} \text{kg} \cdot \text{m}^2$ ]
			$x_G'$ [m]	$z_G'$ [m]		
1	Trunk	0,4874	0,2282	0	39,72	0,467600
2	Head	0,3861	0,1688	0,03892	5,3791	0,022750
3	Right arm	0,3154	0,1460	0	2,0199	0,012520
4	Right forearm	0,3739	0,1728	0	2,4156	0,010250
5	Left arm	0,3154	0,1460	0	2,0199	0,012520
6	Left forearm	0,3739	0,1728	0	2,4156	0,010250
7	Right thigh	0,4143	0,1536	0	9,6969	0,134400
8	Right shank	0,4190	0,1691	0	4,0984	0,056690
9	Right hindfoot	0,1475	0,0328	-0,02732	1,2201	0,005262
10	Left thigh	0,4144	0,1536	0	9,6969	0,134400
11	Left shank	0,4190	0,1691	0	4,0984	0,056690
12	Left hindfoot	0,1475	0,0328	-0,02732	1,2201	0,005262

**Table 2. Anthropometric data for the 2D model with twelve segments.**

After some data processing, a set of fourteen independent coordinates is determined: the hip ( $P_4$ ) Cartesian coordinates together with the angular variables shown in Figure 5 (right).

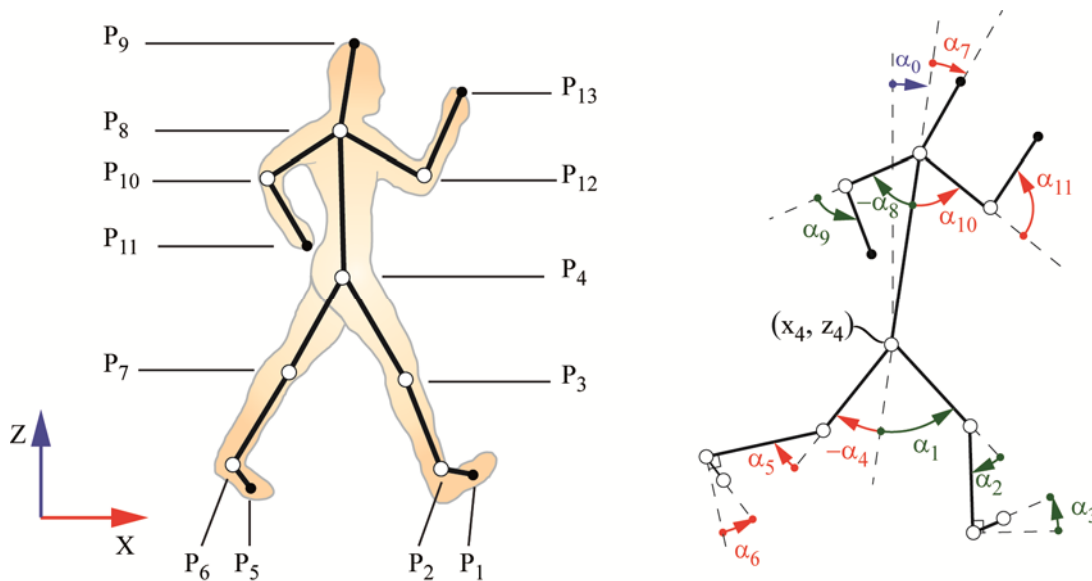


**Figure 5. Points and angles used to define the configuration of the planar model.**

This information together with the force plate measurements are the data input to the system. File “input.txt” contains the temporal evolution of the degrees of freedom (the independent coordinates defined above), the force plate information (rough data) and the position histories of the markers. Column 1 contains the captured time from 0 to 1.56 s with an increment of 0.01 s. Columns 2 and 3 contain the Cartesian coordinates of point  $P_4$ . Columns 4 to 15 contain the angular coordinates from  $\alpha_0$  to  $\alpha_{11}$ , as shown in Figure 5. Columns 16, 17 and 18 contain the contact force from force plate 1 (see Figure 1), and columns 19, 20 and 21 provide the moment components of the contact wrench about the centre of force plate 1. The same values are gathered in columns 22 to 27 for force plate 2.

Finally, the 3D positions of the markers are stored in columns 28 to 139: columns 28, 29 and 30 provide the value of the X, Y and Z Cartesian coordinate of marker M1, respectively. Using this criterion, all the positions of the markers are collected from M<sub>1</sub> to M<sub>37</sub>, as can be seen in Table 3.

t [s]	Kinematics						Force Plates			Markers		
	P <sub>4x</sub> [m]	P <sub>4z</sub> [m]	α <sub>0</sub> [rad]	α <sub>1</sub> [rad]	...	α <sub>11</sub> [rad]	F <sub>x</sub> [N]	...	M <sub>z</sub> [Nm]	M <sub>1x</sub> [m]	...	M <sub>37z</sub> [m]
0,00	-0,816	0,871	0,155	0,616	...	1,099	9,749	...	0,078	-0,325	...	0,034
0,01	-0,806	0,870	0,157	0,618	...	1,103	1,378	...	0,101	-0,320	...	0,033
...												
1,56	0,844	0,907	-0,04	0,298	...	1,082	0,142	...	-0,210	1,149	...	0,033

Table 3. "Input.txt" data.

The obtained results show the inverse dynamic wrenches calculated during phases II, III and IV. The results file ("results.txt"), contains the contact reactions at each foot (F<sub>1</sub>, M<sub>1</sub>, F<sub>2</sub>, M<sub>2</sub>) and the joint torques (τ<sub>1</sub>, ..., τ<sub>11</sub>), as shown in Table 4. The first column contains again the array of time sampling points. Note that the index of the joint torques τ<sub>i</sub> is the same as the angle index α<sub>i</sub> (see figures 5 and 6).

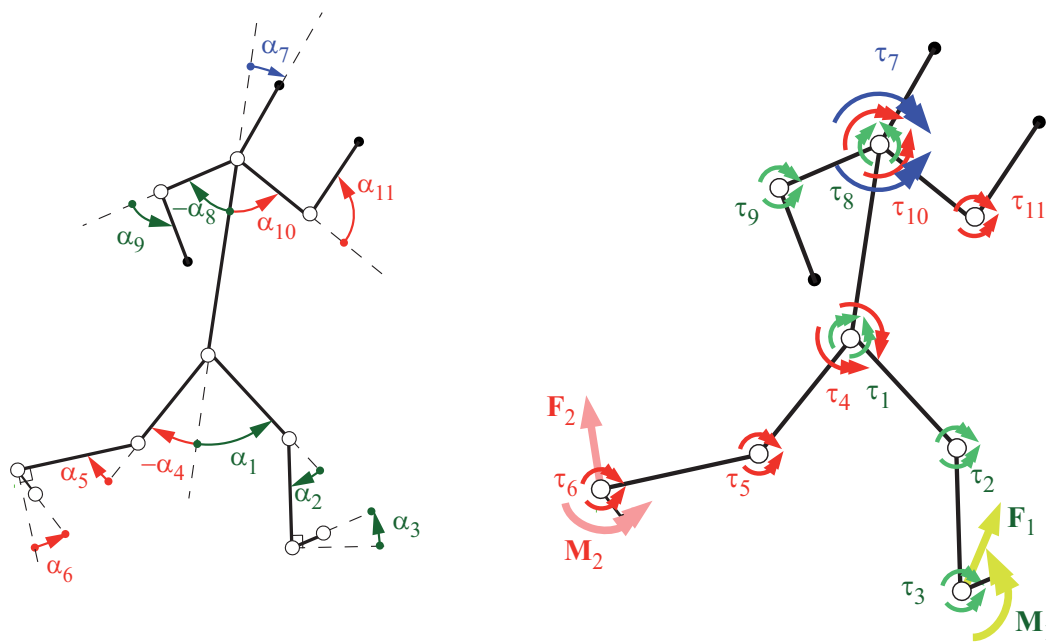
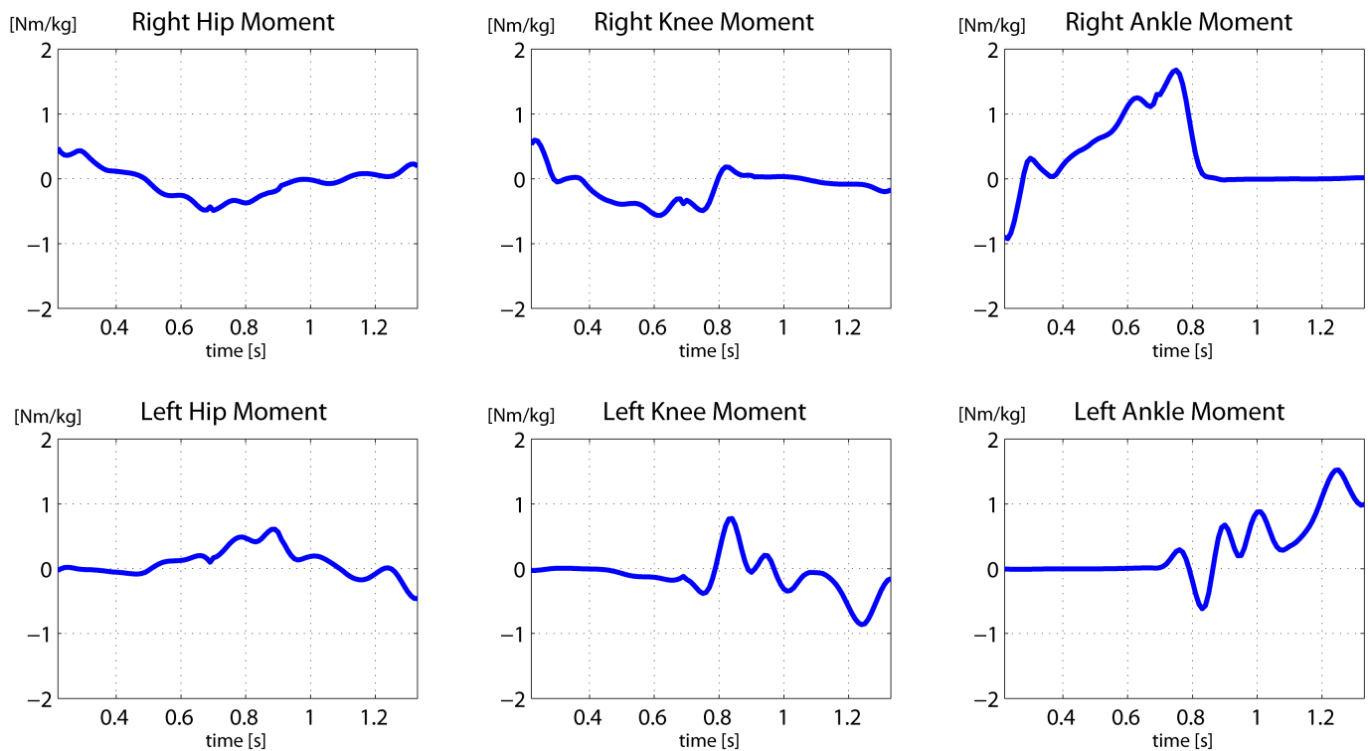


Figure 6. Joint forces and torques representation.

t [s]	F <sub>x1</sub> [N]	F <sub>z1</sub> [N]	M <sub>1</sub> [Nm]	F <sub>x2</sub> [N]	F <sub>z2</sub> [N]	M <sub>2</sub> [Nm]	τ <sub>1</sub> [Nm]	...	τ <sub>11</sub> [Nm]
0,22	-40,09	784,07	75,19	0	0	0	39,87	...	-2,02
0,23	-38,08	792,83	77,39	0	0	0	33,91	...	-1,99
...									
1,33	0	0	0	97,32	817,57	-83,27	16,56	...	-2,94

Table 4. Obtained wrenches during phases II, III and IV.

Figure 7 shows the lower limb joint torques. Note that, in order to be compatible with other experimental results, these torques have been divided by the total body mass of the subject (84 kg), the moment per unit body mass is represented [Nm/kg].



**Figure 7. Lower Limb Joint Torques.**

All the input data and also the output results have been uploaded, so that the user can compare the obtained forces and torques using his own method for inverse dynamic analysis of gait. The specific method applied to obtain the joint torques is detailed in the compressed miscellaneous file.

The data can be used to perform a forward dynamics simulation, too. Finally, visual information regarding the motion is available in videos “3D.avi” and “2D.avi”.